

DESIGN OF THE BEAM TRANSFER LINE MAGNETS FOR HIE-ISOLDE

J. Bauche, A. Aloev, CERN, Geneva, Switzerland

Abstract

This paper describes the design of the beam transfer line magnets of the HIE-ISOLDE facility. The technical solutions selected to face the challenges associated with the machine requirements are presented, and the final design parameters and field quality are reported.

INTRODUCTION

ISOLDE, the Isotope Separator On-Line, is a world-leading facility dedicated to the production and study of a large variety of radioactive nuclei, in operation since 1967 at CERN in Geneva, Switzerland. To extend the physics program, the post accelerator is upgraded to High Intensity and Energy (HIE-ISOLDE [1]) by replacing a part of the normal conducting accelerating structure with a superconducting linear accelerator capable of accelerating beams of mass-to-charge ratios from 2 to 4.5 at energies from 0.3 up to 10 MeV/u. The beam is distributed to three experimental stations through the new High Energy Beam Transfer lines (HEBT) for which new magnets have been tailor-designed. An overview of the machine layout is given in Figure 1.

This paper reports on the technical choices made in the design of these magnets to meet the machine requirements.

MACHINE LAYOUT

The new superconducting LINAC is constituted of four low- β and two high- β cryomodules housing quarter wave resonator cavities and solenoids, in between of which are hosted compact dual plane corrector magnets and beam instrumentation devices. Downstream, after a matching section, the main transfer line adopts a regular lattice with quadrupole doublets up to each experimental line which switches the beam through a 90° double-bend-achromat lattice made of a single quadrupole mirroring the dispersion functions of surrounding dipoles. A final focussing section completes each line to adapt the focal point to the installed experiment. All magnets are powered with individual power converters, in DC current.

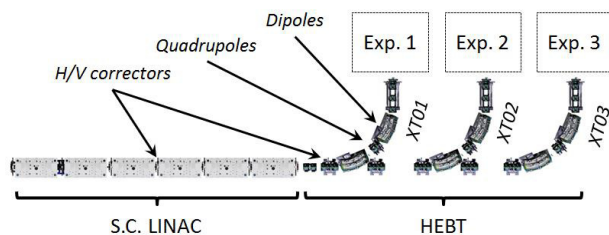


Figure 1: Layout of the HIE-ISOLDE facility.

DIPOLES

Magnetic Circuit

The 1.8 m bending radius and 45° bending angle set by the layout induce a beam trajectory sagitta of 157 mm. This has imposed a curved construction to reduce by approximately a factor of two the overall transverse size of the magnet with respect to a straight design.

Considering the switching function required for the first dipoles of the first two beam lines, the yoke has a C-shape to avoid the straight vacuum chamber of the non-deflected beam to cross the return yoke. This is also convenient to avoid the mechanical imperfections of a split yoke assembly and to allow an easy access for the integration of the coils and of the chamber. The use of laminated steel, helpful to better control and homogenise the magnetic properties along the yoke, is well adapted to this construction. The lamination packs are glued and reinforced with pure iron [2] 40 mm thick end plates and welded tension plates on the sides. As no pulsed operation mode is foreseen, a low silicon content electrical steel is used (M1400-100 A [3]), which has excellent magnetic properties.

The C geometry is built with a constant width of 210 mm sufficient to limit the flux density to 1.5 T in average over the return yoke. In the pole region, 23° tapering's reduce this width to 180 mm, leaving 1.4 times the aperture size on both sides of the Good Field Region (GFR). This is sufficient by itself to achieve a 10^{-3} field quality range. Nonetheless, small shims 0.38 mm x 28.5 mm are added in the pole profile extremities to further improve the design field quality.

The magnet cross-section is illustrated in Figure 2.

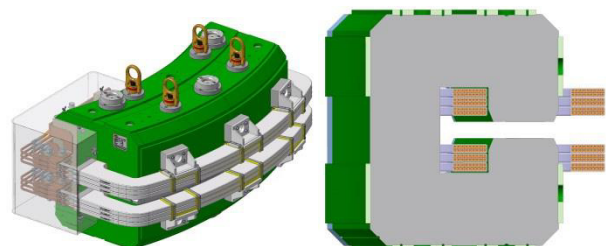


Figure 2. Dipole, isometric view (left), simplified cross-section (right).

The pole face rotation of half the bending angle induced by the laminated construction is kept to provide some focusing in the vertical plane, and keep the yoke construction simple. The magnetic length on each side of the beam axis is adjusted in 3D with the end shims mentioned earlier hosted in slots of the end plates, shaped with the help of magnetic simulation in Opera [4]. These

shims are removable on each magnet to allow corrections after magnetic measurements, if required. The design field quality ends up well inside the $\pm 5 \cdot 10^{-4}$ range requested by the beam optics, with a sufficient margin for manufacturing tolerances. The design normalized integrated field harmonics are presented in Figure 3.

Electrical and Hydraulic Circuits

The magnet electrical circuit is optimized for the use of an existing 500 A power converter. The current is carried in a series of 108 turns distributed along six identical double layer racetrack coils made of hollow copper conductor insulated with vacuum potted epoxy resin reinforced with glass-fibre.

The impedance of the hydraulic circuit is optimized for operating at the nominal differential pressure of the demineralized water distribution network of the facility (10 bars). The conductor cooling duct size, and the parallel connection scheme of the coils are designed to match a ± 4 bars operational window, while staying in reasonable values of water velocity, temperature, and Reynolds number [5].

The dipole main parameters are reported in Table 1.

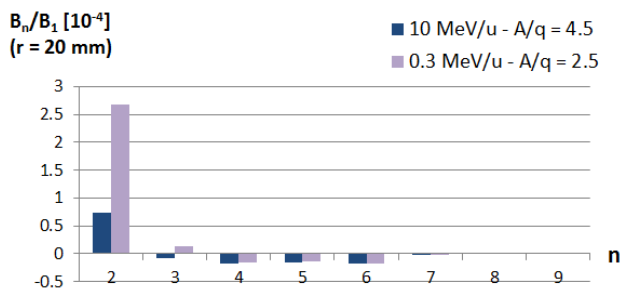


Figure 3. Computed integral field normalized harmonics of dipole at $r_{ref} = 20$ mm.

Table 1: Design Parameters of Dipole Magnets

| Parameter | Units | Value |
|--------------------------------------|------------|-------------------------|
| Number of magnets | | 6 |
| Peak field in centre | T | 1.2 |
| Allowed integrated field error | | $\pm 5 \cdot 10^{-4}$ |
| Magnetic aperture | mm | 50 |
| Magnetic length | mm | 1414 |
| Bending radius | m | 1.8 |
| Bending angle | deg | 45 |
| Conductor dimensions | mm | $\square 10; \text{Ø}6$ |
| Nominal current | A | 423 |
| Magnet resistance (20°C) | m Ω | 100 |
| Magnet inductance | mH | 113 |
| Cooling flow ($\Delta p = 10$ bars) | l/min | 23 |

QUADRUPOLES

Magnetic Circuit

A single design covers the requirements of all magnets in the regular lattice and matching sections of the HEBT.

The yoke is made of a bolted 4-fold symmetric assembly to allow the integration of the coils. Similarly to the dipoles, the yoke quadrants are made of glued low silicon content grade laminations (1300-100 A [3]), here reinforced with pure iron [2] 12.5 mm end plates and longitudinal tie rods.

In the return yoke, enlarged mating surfaces provide a stable contact between quadrants with a large lever arm to ensure a correct orientation of the poles. The poles are straight to host racetrack coils, ending with 18.9° tapering's trimmed by short reference surfaces parallel to the mating faces, which are convenient to perform dimensional checks during assembly. In the central aperture, the pole profile is of the classical hyperbolic shape of equation $2xy = r^2$, surrounded by shims to optimize the 2D field quality. This effort is completed by the cancellation of the integrated dodecapole with an end chamfer of 3.5 mm calculated in Opera [4]. This brings the integral field error below the 10^{-3} level required by the beam optics, with a comfortable margin. The magnet cross-section is illustrated in Figure 4; the design normalized integrated field harmonics are presented in Figure 5.

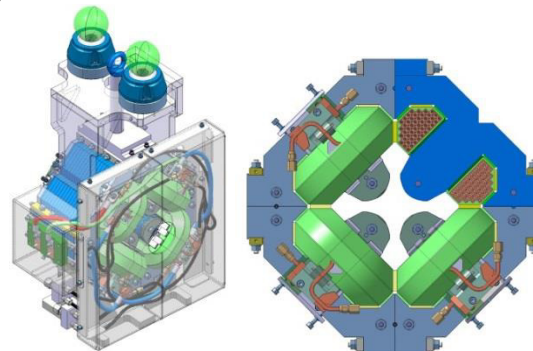


Figure 4. Quadrupole, isometric view (left), and simplified front view with quadrant cross section (right).

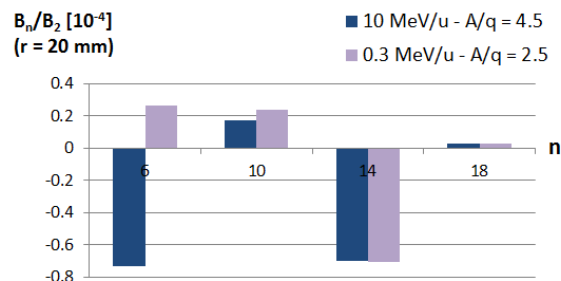


Figure 5. Computed integral field normalized harmonics of quadrupole.

Electrical and Hydraulic Circuits

The optimal matching with the power converter characteristics is obtained with four 48 turn coils powered in a series circuit. The technology is the same as for the

dipole coils. The hydraulic impedance of the cooling circuit is optimized, in a similar way as explained above, with two parallel branches feeding two coils each. The quadrupole main parameters are shown in Table 2.

Table 2: Design Parameters of Quadrupole Magnets

| Parameter | Units | Value |
|--------------------------------------|-------|------------------------|
| Number of magnets | | 24 |
| Peak field gradient in centre | T/m | 24 |
| Allowed integrated gradient error | | $\pm 1 \cdot 10^{-3}$ |
| Magnetic aperture diameter | mm | 50 |
| Magnetic length | mm | 209 |
| Conductor dimensions | mm | $\square 6; \text{Ø}4$ |
| Nominal current | A | 142 |
| Magnet resistance (20°C) | mΩ | 105 |
| Magnet inductance | mH | 30 |
| Cooling flow ($\Delta p = 10$ bars) | l/min | 2.6 |

DUAL PLANE CORRECTORS

The challenging requirements on the corrector magnets total length (92 mm) and field strength (6 mT·m) [6] are met with an original design of window-frame magnet where the coil windings are oriented orthogonally w.r.t. the magnet longitudinal axis, as shown in Figure 6. This allows maximizing the occupation of the longitudinal space exclusively with the yoke iron and the coil conductors. Most of the field strength is provided by the stray field, some 30% of which is absorbed by adjacent quadrupoles in the HEBT. Though an air-cooled coil design could provide the required ampere-turns in the LINAC [7], a stronger water-cooled single design is adopted to cover the LINAC and HEBT needs. The inner corners of the solid pure iron [2] magnetic circuit are trimmed to create poles, and a trapezoidal cross-section is adopted for the coils to limit field errors (Figure 7.). The hydraulic and electrical parameters are optimized to the power converters and cooling water network characteristics, in a similar way as explained above. The magnet parameters are shown in Table 3.

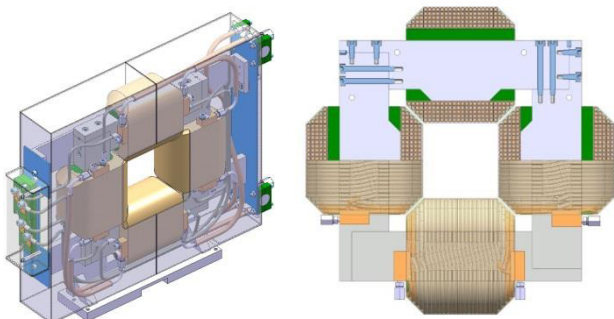


Figure 6. Corrector magnet, isometric view (left), simplified front view with cut out of top half (right).

Table 3: Design Parameters of Corrector Magnets

| Parameter | Units | Value |
|--------------------------------------|-------|--------------------------|
| Number of magnets | | 15 |
| Integrated field in centre | mT·m | 9.1 |
| Allowed integrated field error | % | ± 2 |
| Free aperture | mm | 92 x 92 |
| Magnetic length | mm | 258 |
| Conductor dimensions | mm | $\square 4; \text{Ø}2.5$ |
| Nominal current | A | 48 |
| Resistance (per plane, 20°C) | mΩ | 109 |
| Inductance (per plane) | mH | 10 |
| Cooling flow ($\Delta p = 10$ bars) | l/min | 0.4 |

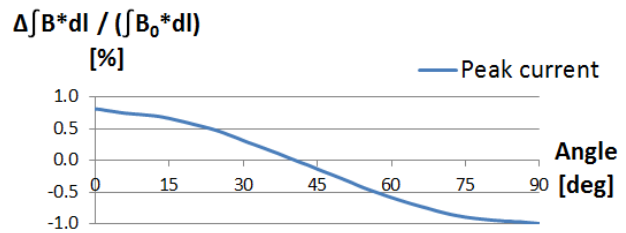


Figure 7. Computed integral field relative error at $r_{ref} = 20$ mm, at peak current.

ACKNOWLEDGMENTS

The authors would like to thank E. Solodko, M. Timmins, and C. Mucher for their contributions in the mechanical design of the magnets, as well as A. Milanese and D. Tommasini for helpful discussions.

REFERENCES

- [1] K. Riisager, “The HIE-ISOLDE project”, *AIP Conf. Proc. 1012*, 2008, pp 106 – 110.
- [2] ARMCO Grade 4 from A.K. Steel International [Online]. Available: <http://www.aksteel.eu/en/1-products/0-ingot-iron>
- [3] AFNOR, “Cold rolled non-oriented electrical steel sheet and strip delivered in the fully processed state” NF EN 10106:2007, 1st Issue-2007-12-P.
- [4] OPERA 3D / TOSCA form Vector Fields [Online]. Available: <http://www.vectorfields.co.uk>
- [5] D. Tommasini, “Practical Definitions and Formulae for Normal conducting Magnets”, CERN Internal Note 2011-18, EDMS 1162401, September 2011.
- [6] M. A. Fraser, M. Pasini, “Misalignment and error studies of the high energy section of the HIE-ISOLDE Linac”, CERN Internal Note, October 2009.
- [7] J. Bauche, “Compact Inter-Cryomodule Combined Corrector Magnets for the HIE-ISOLDE Facility at CERN”, *IEEE Transactions on Applied Superconductivity*, vol. 22, No. 3, June 2012.